Journal of Solid State Electrochemistry (2024) 28:411–418
https://doi.org/10.1007/s10008-023-05784-4

SHORT COMMUNICATION

Polyvinylpyrrolidone (PvP) adsorbs on and interacts with biomembrane-like layers

Bethany Crow[1] · William E. Stokes[1] · Nikil Kapur[2] · Marti Busquets Fite[3] · Andrew Nelson[1]

Received: 30 June 2023 / Revised: 14 November 2023 / Accepted: 17 December 2023 / Published online: 28 December 2023
© The Author(s) 2023

Abstract

This communication describes an initial study into the interaction of solution polyvinylpyrrolidone (PvP) with electrode-supported monolayers of dioleoyl phosphatidylcholine (DOPC). Experiments were carried out in phosphate buffered saline (PBS) at pH 7.4, and solutions were screened on a DOPC-coated microfabricated Hg/Pt electrode in flow cell. The effect of the PvP interaction on the form of rapid cyclic voltammograms (RCV) was recorded at 40 Vs^{-1}. It was found that the PvP-DOPC interaction is strongly dependent on PvP chain length. For shorter chain lengths, the interaction is linearly related to PvP concentration whereas at longer chain lengths, the interaction is Langmuirean; however, the interaction RCV in all cases is representative of adsorption. Both the affinity constant, K_2, and the limit of detection (LoD) are extracted from these plots, and these values are inversely related to each other. Plots of log K_2 and –log LoD versus the monomer segment number (PvP_m) fit a two-term equation consisting of a power term and an exponential term. Plots of (log K_2)/PvP_m versus PvP_m are near reciprocal showing that there is 'looping' of the chains on the DOPC surface during the adsorption process. The results fit a model of entropically driven adsorption at short chain lengths and enthalpically driven adsorption at longer chain lengths the latter assumedly due to non-covalent interactions between the PvP chains on the DOPC surface.

Keywords Dioleoyl phosphatidylcholine monolayers · Rapid screening · Polyvinylpyrrolidone · Polymer adsorption · Affinity constant · Limit of detection

Introduction

Polyvinylpyrrolidone (PvP) has many applications [1, 2]. These arise from its implicit non-ionic polymer [3] properties, apparent inert behaviour and lack of activity towards biological organisms and material [2]. As a result, PvP has been widely used for stabilising nanomaterial dispersions [4, 5] especially where they have a medical use in applications like drug delivery [6]. Its stabilising property comes from the fact that it adsorbs on and coats nanomaterial and, being neutrally charged, minimises aggregation within the material dispersions [4, 5]. PvP consists of monomer units of *N*-vinylpyrrolidone (*N*-vP) [2] (Fig. 1). The tendency of *N*-vP to form non-covalent interactions with biological material will be small since the monomer units have one H- bond acceptor as the carbonyl bond and a log *P* value of 0.37. Log *P* is defined as the log octanol–water partition coefficient (log K_{OW}) of a compound. This is a thermodynamic quantity relating to the partitioning of a compound between octanol and water. It has a standard use for defining the lipophilicity of pharmaceuticals and toxicants [7]. Commensurate with the relatively low log *P* value of the PvP monomer, PvP is hydrophilic and water soluble, and in aqueous solution, it remains in a coiled configuration [3]. The PvP polymer adsorbs on surfaces [8–10] and this property, and its interaction with other surfactants [3] and compounds in solution [11] has been variously studied in particular in relation to the adsorptive behaviour of polymers in general. In fact generally the adsorption of polymers on surfaces has attracted a lot of interest [12–18]. Many studies agree that polymer adsorption is entropically driven [19]. The main mechanism here is the release of bound water molecules from the solution polymer and the adsorbate surface during

✉ Andrew Nelson
a.l.nelson@leeds.ac.uk

[1] School of Chemistry, University of Leeds, Woodhouse Lane, Leeds LS2 9JT, UK

[2] School of Mechanical Engineering, University of Leeds, Woodhouse Lane, Leeds LS2 9JT, UK

[3] Applied Nanoparticles SL, Vall d'Hebron Institut de Recerca, Passeig de la Vall d'Hebron, 119-129, 08035 Barcelona, Spain

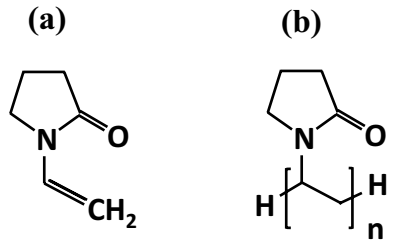

Fig. 1 Structures of **a** *N*-vinylpyrrolidone (*N*-vP) and **b** polyvinylpyrolidone (PvP)

the adsorption process[19]. In the case of the phospholipid surface, this effect could be specially significant in view of the large amount of water molecules associated with the phospholipid polar groups [20] some of which will be displaced. This entropy gain will generally override the entropy loss when the polymer transforms from a 3D to a 2D environment on the adsorbate surface [21–24]. PvP presents an interesting case of polymer adsorption in that the possibility of only selected segments adsorbing leading to a looped or bunched configuration on adsorption can occur [17].

This communication reports a preliminary study on the interaction of PvP with supported phospholipid layers as a function of its chain length. The work has been initiated since many nanomaterial dispersions are coated with PvP [6, 8, 10, 16]. It is instructive therefore to have some knowledge of the effect of the PvP coating on the interaction of the nanomaterial with the lipid layer and indeed its interaction with biological targets. However, as a first step, it is necessary to know how the PvP itself interacts with lipid layers. It is especially important to do this since to date, there have been very few investigations on the interaction of PvP with lipid vesicles [25, 26] and lipid monolayers [27], and on the interaction of Ag nanomaterial coated with PvP with lipid monolayers [28].

Materials and methods

Five samples of PvP of molecular weights, 3.5, 10, 55, 360 and 1300 kD mole^{-1}, were obtained from Sigma-Aldrich, and stock solutions were prepared for electrochemical analysis in 18.2 M.Ωcm Milli-Q water. Each PvP sample is characterised throughout the text by the number of monomer units obtained through dividing the molecular weight of PvP by that of *N*-PvP of 111.14 g mole^{-1} and expressed as PvP_m, i.e. for the five PvP samples as 31, 90, 495, 3239 and 11,697, respectively. The electrolyte used in the electrochemical experiments was 0.0138 mol dm^{-3} NaCl and 0.00027 mol dm^{-3} KCl buffered at pH 7.4 with 0.00119 mol dm^{-3} phosphate (hereinafter in the text referred to as PBS). The PBS was of analytical grade and purchased from Sigma-Aldrich. The microfabricated platinum electrodes (Hg/Pt) used in the electrochemical assay [29, 30] were supplied by the Tyndall National Institute, Ireland. The dioleoyl phosphatidylcholine (DOPC) was obtained from Avanti Polar Lipids Alabaster, AL, USA and was > 99% pure. The DOPC dispersion for electrode coating was prepared by gently shaking DOPC with PBS to give a 0.25 μmole cm^{-3} dispersion. All other chemicals and reagents were of analytical grade and purchased from Sigma-Aldrich.

Apparatus and procedure

For the assay, the fabricated Hg/Pt electrode was contained in a flow cell consisting of a microfluidic flow cell containing the DOPC monolayer supported on a Hg sensing electrode, four automated bespoke syringe pumps enabling storage and transportation of fluids (electrolyte, test sample, phospholipid and water) into the flow cell, a field-programmable gate array (FPGA) data acquisition and control unit used to interface between software and hardware and an ACM Research Potentiostat for electrochemical measurements. A laptop was connected to control the screening platform, interfacing with syringe pumps and the FPGA control unit. The microfabricated electrode was prepared in advance by cleaning in a 1 mol dm^{-3} solution of NaOH in methanol, followed by HCl and Milli-Q water and then dried. Hg was manually deposited on the Pt disc of radius 0.480 mm to give a Hg/Pt electrode. The electrode was mounted as specified in Owen et al. [29]. Subsequently, all samples were deoxygenated (PvP solution, DOPC, electrolyte) with argon gas (Air Products) for a minimum of 30 min. Once purged, three syringes were filled with PvP sample (5 mL), DOPC dispersion (60 mL) and PBS (60 mL), respectively, and connected to tubing. Before any analysis, all tubing was flushed with deoxygenated PBS, and any bubbles were removed from the cell. Turning the potentiostat to run, the system was set to (i) clean with the electrochemical rejection of the previous used monolayer, (ii) deposit DOPC from dispersion, (iii) test the monolayer integrity in PBS and (iv) screen the sample solution as described previously in refs [29, 30] and in Table S1 in the SI. Upon single-sample completion, the sample tubing was flushed with PBS (5 mL). This was the analytical cycle for each sample. Samples were measured at increasing concentrations of one PvP sample, then switching to the next PvP sample. The sample syringe was replaced with every repeat of the same sample and between PvP sample solutions. All measurements were carried out in triplicate, and five PvP concentrations were screened for each PvP chain length sample. All fits to the data were carried out using the program IGOR Pro 9, and coefficients and their errors (SD%) for all fits are listed in Tables S2 and S3 in the SI.

Results and discussion

The system of a phospholipid monolayer adsorbed on a mercury electrode as a biomembrane model has been developed over four decades [31–33]. It has had fundamental biophysical applications for example in analysing ion channel [34], co-enzyme activity [35] and phospholipid behaviour in electric field [36–38]; however, its predominant practical implementation has been used in modelling the biomembrane activities of molecular [39–41] and nanoparticle species [41, 42]. Originally, a modified Langmuir–Blodgett technique was used for depositing the phospholipids on a hanging mercury drop electrode [32, 33]. Since these techniques were totally inappropriate for rapid and routine screening, the electrode was re-configured as a microfabricated Hg on Pt film electrode [29, 30, 43], and the phospholipid deposition was enabled from vesicles in a flow cell [29, 30]. In this study, a DOPC monolayer is deposited on the Hg electrode on the prepared Pt support and scanned at 40 Vs^{-1} from − 0.4 to − 1.2 V referred to throughout the text as rapid cyclic voltammetry (RCV) [29, 30, 43] (see Table S1 in the SI). The layers undergo potential-induced phase transitions characterised by two sharp capacitance current peaks (voltammetric), 1 and 2, respectively, as shown in Fig. 2 [29, 30, 43]. These two peaks correspond to the penetration of electrolyte into the layer and the reorganisation of the monolayer to form bilayer patches, respectively [36–38]. Changes in these capacitance peaks represent changes in the structure of the monolayer [29, 30, 43]. The interaction of the test substance with the monolayer selectively and systematically influences the capacitance-current potential profile [39–42]. An interaction of the test substance with the polar groups of the DOPC is reflected in a depression of the two peaks [39, 40] while an increase in the baseline of the capacitance current reflects the association of a polar compound with the apolar region of the DOPC layer and/or its disruption [38–41]. The reason for the latter effect is that the low value of baseline capacitance current is representative of the ordered DOPC layers on the electrode with the low dielectric apolar lipid tails adjacent to the electrode surface. When this low dielectric region is penetrated by a higher dielectric compound, the average dielectric constant of this region increases leading to an increase in the baseline capacitance current [39–41]. A potential shift in the capacitance current peaks indicates a change in the potential profile across the layer caused by the interaction of the compound with the layer [40, 44]. A monolayer disordering is shown as a broadening of the peaks [40, 41]. The screening results from this sensor platform have recently been shown to be related to biomembrane damage in in vitro cell cultures [45]. Other research groups have followed a similar approach, but not in rapid *online* screening format [46–48].

The RCV plots in this study show a PvP interaction with the DOPC monolayer as a depression of the RCV capacitance current peaks (see Fig. 2). This peak depression directly corresponds to the presence of adsorbed species on the monolayer surface [42], and the extent of peak depression is linearly related to the coverage [42, 49]. In order to obtain a quantitative estimate of the effect of each compound on the DOPC layer, affinity constants (K_2) and limits of detection (LoD) for PvP in PBS are estimated from the PvP calibration curves. The configuration of the RCV following the interaction displays exactly the same change in form with increasing PvP concentration irrespective of the PvP chain length. Significantly, with increasing PvP solution concentrations, the interactions showed the RCV capacitance peak currents as successively depressed with no potential shift, no peak broadening and no increase in the capacitance baseline current. The absence of an increase in the capacitance minimum current indicates that the PvP does not penetrate the DOPC layers with the interaction remaining at an adsorptive superficial level on the DOPC layer. Further evidence for this comes from the configuration of the calibration curves (capacitance peak current 1 suppression % versus PvP concentration) which are linear for lower PvP_m values of 31 and 90 but Langmuirean [50] for higher PvP_m values of 495, 3239 and 11,697 as shown in Figs. 3

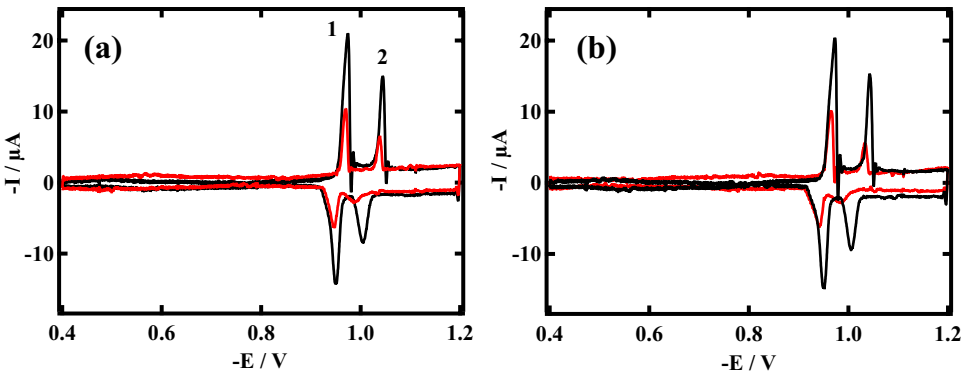

Fig. 2 RCVs at 40Vs^{-1} of DOPC on microfabricated Hg/Pt electrode in PBS at pH 7.4 (black line) and with added **a** 5 and **b** 0.18 µmole dm^{-3} of PvP_m 31 and 3239, respectively (red line). Capacitance current peaks 1 and 2 labelled on (**a**)

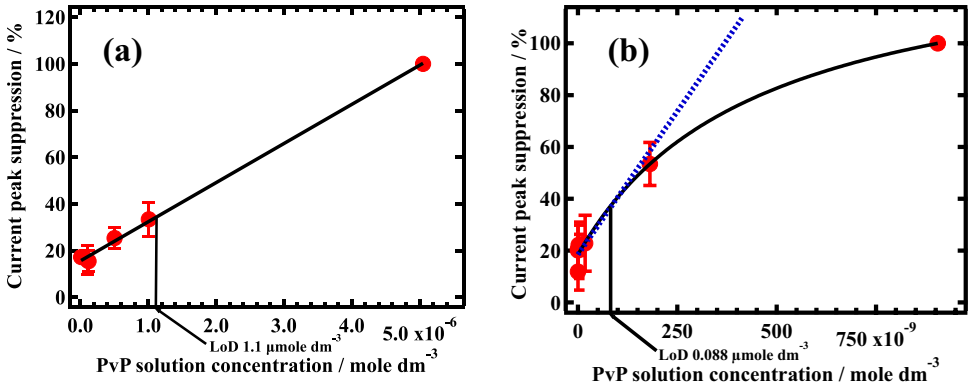

Fig. 3 Plots of % capacitance current peak 1 suppression versus solution concentration of PvP with LoD value indicated on horizontal axis **a** 90 and **b** 3239 PvP_m, slope 'c' indicated by blue stippled line

and S1. This shows intuitively that PvP surface coverage becomes limiting at longer chain lengths.

The linear plots are fitted to Eq. (1):

$$Y = a + cX \tag{1}$$

The Langmuirean plots [50] are fitted to Eq. (2):

$$Y = a + \left[bX/(100 + cX)\right] \tag{2}$$

Y is the % current peak depression, X is the solution concentration of PvP and 'a' is the intercept due to some depression of the control current peak during the assay. The slope 'c' is shown on the calibration plots in Figs. 3a, b. The coefficients and their errors are displayed in Table S2 in the SI. Although the fits are good and the coefficients are reasonable, there are large errors on one of the calibration points of the 11,697 PvP_m polymer. Since this communication is only focused on the sensor element response to the lower PvP solution concentrations as a molecular initiation event (MIE) [51], the response plots at higher PvP concentration are not of concern here and will be studied more comprehensively in further work. The LoD metric of the PvP affinity for the DOPC monolayer is the lowest significant solution concentration of PvP, which can structurally modify the DOPC layer and is estimated from 3 times the standard deviation of the DOPC capacitance peak 1 current corresponding to the PvP solution concentration on the appropriate calibration curve [39, 40]. The LoD error is taken from the error of the slope coefficient for the linear plot and the errors associated with both coefficients for the Langmuir plots, respectively. The relation of the LoD to the calibration curves is shown in Fig. 3. The metric K_2 is defined as the slope 'c' of Eq. (1) in Fig. 3a and the slope 'c' of Eq. (2) in Fig. 3b both divided by 100 to give the fractional depression of the capacitance peak current 1 per unit PvP solution concentration. K_2 is taken to represent the affinity constant [50] of PvP for the DOPC surface. This assumption is justified from the experimental data since log K_2 linearly correlates with − log LoD for all polymer chain lengths (see Fig. 4a), and − log LoD has been an established measure of the affinity of a compound for the phospholipid layer [39, 40]. The empirical equation for the relation between log K_2 and –log LoD can be extracted from the fit in Fig. 4a as:

$$\log K_2 = -0.91 - 1.03.\log \mathrm{LoD} \tag{3}$$

The following can be derived from the linear relation between log K_2 and − log LoD:

$$K_2 = 1/\left(8.1\mathrm{LoD}^{1.03}\right) \tag{4}$$

The relationship of K_2 with the free energy of adsorption (ΔG) will ideally follow the formal equation, ΔG = − RT

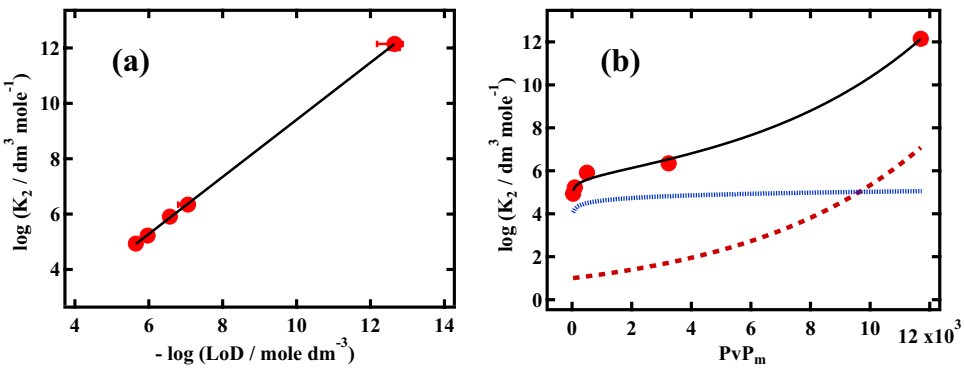

Fig. 4 **a** Plot of log K_2 versus − log LoD values derived from % capacitance current peak 1 suppression versus solution PvP concentration calibrations and **b** plot of log K_2 versus PvP_m (red circles) fitted to Eq. (5) (black line), Eq. (5) terms: exp $(1.7\times10^{-4}.PvPm)$ (red dashed line) and 3.58. $PvP_m^{0.037}$ (blue stippled line), versus PvP_m

ln K_2 [50] so log K_2 is an effective metric relating to the adsorption energy and is used as such in this study.

Plots of log K_2 versus PvP_m are displayed in Fig. 4b and show an increase which is steepest for the shortest PvP chains and is curvilinear for the longer chains. The plot can be empirically fitted to the following:

$$\log K_2 = \exp\left(1.7 \times 10^{-4} \times PvP_m\right) + 3.58.PvP_m{}^{0.037} \quad (5)$$

and similarly for − log LoD:

$$-\log \mathrm{LoD} = \exp\left(1.6 \times 10^{-4} \times PvP_m\right) + 3.91.PvP_m{}^{0.037} \quad (6)$$

Interestingly, the LoD for a single unit of *N*-vinylpyrrolidone (*N*-vP) can be estimated from Eq. (6) as 12.3 µmole dm^{-3} which is reasonable for such a single-saturated ringed molecular structure as reported in previous publications [39, 40]. If each monomer unit contributes a linear increase to the affinity of the combined polymer for the DOPC, a constant value of log K_2 per monomer number in the polymer would be expected. In fact if (log K_2)/PvP_m is plotted against PvP_m (Fig. 5a), it exhibits a near reciprocal decrease which fits Eq. (5). Significantly, Eq. (5) fits the data better at higher PvP_m than a reciprocal fit shown in the inset to Fig. 5a. This decrease in adsorption energy for individual units with increase in chain length can indicate two effects:

(1) Only selected monomer units are adsorbing on the DOPC surface allowing sections of the chain to remain attached as loops [17] but not adsorbed.
(2) The length of the chain affects the affinity of a monomer unit for the surface.

If the first factor is critical, it can lead to a near reciprocal decrease in log K_2 with PvP_m as the 'looping' of chains at the surface becomes more extensive proportionately with the chain length. In terms of the second factor, it is instructive to take a preliminary look at the thermodynamics of the adsorption in order to further understand the form of the log K_2 vs PvP_m relationship.

Eqs (5) and (6) show that the affinity of the PvP for the DOPC is divided into two terms. These are plotted out in Fig. 4b for log K_2. These terms fit a model whereby a combination of entropic and enthalpic forces drive the polymer adsorption. The exponential term may be identified with the enthalpic contribution of this model showing an increase from a small value to a higher value at long chain lengths. The small value at short chain lengths is consistent with the low propensity of the PvP monomer unit to bind with the DOPC surface having only one H-bond acceptor group which would interact with the positively charged DOPC choline moiety and a low log *P* value of 0.37 which reflects a weak tendency of the molecule to partition into an organic phase such as lipid. The exponential increase in this term with chain length reflects the increasing tendency for the PvP chains to interact with each other on the DOPC surface as the chains become longer. Such an interaction is consistent with the increasing entanglement of 'looped' chains on the DOPC surface as the chains become longer and is commensurate with the finding that solution PvP has a propensity for self-assembly [52]. The power term in Eqs. (5) and (6) can represent the entropic contribution to the adsorption model due to dissociation of water molecules from PvP and from the DOPC surface [20] following PvP adsorption. This necessarily increases with increasing chain length but at longer chain lengths, it levels off due to the increasing relative significance of the entropy loss due to change in PvP configuration from 3 to 2 dimensions.

The PvP adsorption effects can be seen more clearly if the K_2 value is divided by PvP_m. Conceptually, this normalises the adsorption affinity constant to the PvP's monomer segment instead of the polymer. Figure 5b shows a plot of log (K_2/PvP_m) as a function of PvP_m. A steep

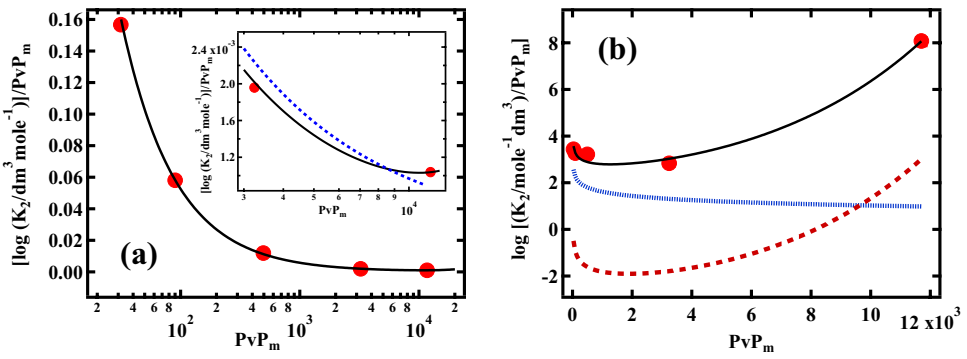

Fig. 5 **a** Plot of (log K_2)/PvP_m versus PvP_m (red circles) fitted to rearranged Eq. (5) (black line) with inset of same plot at high PvP_m showing reciprocal fit [(log K_2)/PvP_m = $3 \times 10^{-4} + 4.1.PvP_m{}^{-0.95}$] to plot as blue dashed line. **b** Plot of log (K_2/PvP_m) versus PvP_m (red circles) fitted to Eq. (5) − log PvP_m (black line) with terms: exp (1.7×10^{-4}. PvPm) − log PvP_m (red dashed line) and $3.58.PvP_m{}^{0.037}$ − log PvP_m (blue stippled line), versus PvP_m

decrease in log (K_2/PvP_m) with PvP_m is observed followed by a curvilinear increase at longer chain lengths. Equation (5) – log PvP_m fits the data and the separate terms minus log PvP_m, respectively, have been plotted versus PvP_m. Both terms show steep decreases at lower PvP_m, but only the exponential term increases at longer chain lengths. These results fit the model whereby both the monomer normalised entropic and enthalpic contributions are significantly affected by the 'looping' of the polymer on the surface at shorter chain lengths. At longer chain lengths, the enthalpic contribution from the association of polymer on the DOPC surface becomes significant. The results and the model proposed in this work are consistent with the state-of-the-art findings on polymer adsorption where the adsorption is an interplay between entropic and enthalpic forces [53–55].

Conclusions

Aqueous PvP interacts with electrode-supported phospholipid layers of DOPC. This interaction is strongly dependent on chain length. For shorter chain lengths, the interaction is linearly related to PvP solution concentration whereas at longer chain lengths, the interaction is Langmuirean; however, the interaction voltammogram in all cases is representative of an adsorption process. Both the affinity constant, K_2, and the limit of detection, LoD, are extracted from these plots, and log K_2 and – log LoD are directly related to each other. Plots of log K_2 and – log LoD versus the monomer segment number, PvP_m, fit a two-term equation consisting of a power term and an exponential term. A plot of (log K_2)/PvP_m versus PvP_m is near reciprocal showing that there is 'looping' of the chains on the DOPC surface during the adsorption process. The results fit a model whereby the adsorption is entropically driven at short chain lengths but at longer chain lengths, non-covalent interactions between the chains on the DOPC surface can assist in promoting adsorption.

Supplementary Information The online version contains supplementary material available at https://doi.org/10.1007/s10008-023-05784-4.

Author contribution All authors contributed to the study conception and design. Material preparation, data collection and analysis were performed by AN, BC and MBF. WES modified the screening platform with supervision from NK, and, WES supervised the experiments. The first draft of the manuscript was written by AN, and all authors commented on previous versions of the manuscript. All authors read and approved the final manuscript. NK assisted with the revised version.

Funding This work was funded through the EU Horizon 2020 Programme SABYDOMA Grant agreement No: 862296 and through the UKRI Horizon Europe Guarantee fund Bio-SUSHY Grant reference No: 10056199.

Declarations

Competing interests The authors declare no competing interests.

Open Access This article is licensed under a Creative Commons Attribution 4.0 International License, which permits use, sharing, adaptation, distribution and reproduction in any medium or format, as long as you give appropriate credit to the original author(s) and the source, provide a link to the Creative Commons licence, and indicate if changes were made. The images or other third party material in this article are included in the article's Creative Commons licence, unless indicated otherwise in a credit line to the material. If material is not included in the article's Creative Commons licence and your intended use is not permitted by statutory regulation or exceeds the permitted use, you will need to obtain permission directly from the copyright holder. To view a copy of this licence, visit http://creativecommons.org/licenses/by/4.0/.

References

1. Haaf F, Sanner A, Straub F (1985) Polymers of N-vinylpyrrolidone: synthesis, characterization and uses. Polym J 17:143–152. https://doi.org/10.1295/polymj.17.143
2. Burnett CL (2017) PVP (polyvinylpyrrolidone). Int J Toxicol 36(suppl 2):50S-51S
3. Kamli M, Guettari M, Tajouri T (2019) Structure of polyvinylpyrrolidone aqueous solution in semi-dilute regime: roles of polymer-surfactant complexation. J Mol Struct 1196:176–185. https://doi.org/10.1016/j.molstruc.2019.06.069
4. Mirzaei A, Janghorban K, Hashemi B, Bonyani M, Leonardi SG, Neri G (2017) Characterization and optical studies of PVP-capped silver nanoparticles. Journal of Nanostructure in Chemistry 7:37–46. https://doi.org/10.1007/s40097-016-0212-3
5. Balankura T, Qi X, Fichthorn KA (2018) Solvent effects on molecular adsorption on Ag surfaces: polyvinylpyrrolidone oligomers. J Phys Chem C 122:14566–14573. https://doi.org/10.1021/acs.jpcc.8b03156
6. Ahlberg S, Antonopulos A, Diendorf J, Dringen R, Epple M, Flöck R, Goedecke W, Graf C, Haberl N, Helmlinger J, Herzog F (2014) PVP-coated, negatively charged silver nanoparticles: a multi-center study of their physicochemical characteristics, cell culture and in vivo experiments. Beilstein J Nanotechnol 5:1944–1965. https://doi.org/10.3762/bjnano.5.205
7. Hansch C, Leo A, Hoekman D (1995) Exploring QSAR: hydrophobic, electronic, and steric constants (Vol. 2). Washington, DC: American Chemical Society. p 22
8. Al-Saidi WA, Feng H, Fichthorn KA (2012) Adsorption of polyvinylpyrrolidone on Ag surfaces: insight into a structure-directing agent. Nano Lett 12:997–1001. https://doi.org/10.1021/nl2041113
9. Parnas RS, Chaimberg M, Taepaisitphongse V, Cohen Y (1989) The adsorption of polyvinylpyrrolidone and polyethylene oxide onto chemically modified silica. J Colloid Interface Sci 129:441–450. https://doi.org/10.1016/0021-9797(89)90457-8
10. Lakhwani S, Rahaman MN (1999) Adsorption of polyvinylpyrrolidone (PVP) and its effect on the consolidation of suspensions of nanocrystalline CeO_2 particles. J Mater Sci 34:3909–3912. https://doi.org/10.1023/A:1004678908275
11. Molyneux P, Frank HP (1961) The interaction of polyvinylpyrrolidone with aromatic compounds in aqueous solution. Part 1. thermodynamics of the binding equilibria and interaction forces1. J Am Chem Soc 83:3169–3174
12. Oe N, Hosono N, Uemura T (2021) Revisiting molecular adsorption: unconventional uptake of polymer chains from solution into

sub-nanoporous media. Chem Sci 12:12576–12586. https://doi.org/10.1039/D1SC03770F
13. Liu S, Xu J, Li X, Yan T, Yu S, Sun H, Liu J (2021) Template-free self-assembly of two-dimensional polymers into nano/micro-structured materials. Molecules 26:3310. https://doi.org/10.3390/molecules26113310
14. Linse P, Kallrot N (2010) Polymer adsorption from bulk solution onto planar surfaces: effect of polymer flexibility and surface attraction in good solvent. Macromolecules 43:2054–2068. https://doi.org/10.1021/ma902338m
15. Simavilla DN, Huang W, Vandestrick P, Ryckaert JP, Sferrazza M, Napolitano S (2017) Mechanisms of polymer adsorption onto solid substrates. ACS Macro Lett 6:975–979. https://doi.org/10.1021/acsmacrolett.7b00473
16. Naden BJ (2008) Polymer adsorption to titania surfaces studied by adsorption isotherm, rheology and atomic force microscopy. PhD thesis, Imperial College, University of London, UK
17. Tadros T (2013) Polymer adsorption. In: Tadros, T. (eds) Encyclopedia of colloid and interface science. Springer, Berlin, Heidelberg. https://doi.org/10.1007/978-3-642-20665-8_34
18. O'Shaughnessy B, Vavylonis D (2003) Irreversible adsorption from dilute polymer solutions. Eur Phys J E 11:213–230. https://doi.org/10.1140/epje/i2003-10015-9
19. Kishani S, Benselfelt T, Wågberg L, Wohlert J (2021) Entropy drives the adsorption of xyloglucan to cellulose surfaces–a molecular dynamics study. J Colloid Interface Sci 588:485–493. https://doi.org/10.1016/j.jcis.2020.12.113
20. Disalvo EA, Lairion F, Martini F, Tymczyszyn E, Frías M, Almaleck H, Gordillo GJ (2008) Structural and functional properties of hydration and confined water in membrane interfaces. Biochimica et Biophysica Acta (BBA)-Biomembranes 1778:2655–2670. https://doi.org/10.1016/j.bbamem.2008.08.025
21. Ben-Tal N, Honig B, Bagdassarian CK, Ben-Shaul A (2000) Association entropy in adsorption processes. Biophys J 79:1180–1187. https://doi.org/10.1016/S0006-3495(00)76372-7
22. Gaberle J, Gao DZ, Watkins MB, Shluger AL (2016) Calculating the entropy loss on adsorption of organic molecules at insulating surfaces. J Phys Chem C 120:3913–3921. https://doi.org/10.1021/acs.jpcc.5b12028
23. Király Z, Dékány I (1990) Enthalpy and entropy effects in adsorption and displacement. Colloids Surf 49:95–101. https://doi.org/10.1016/0166-6622(90)80095-L
24. Dauenhauer PJ, Abdelrahman OA (2018) A universal descriptor for the entropy of adsorbed molecules in confined spaces. ACS Cent Sci 4:1235–1243. https://doi.org/10.1021/acscentsci.8b00419
25. Dékány G, Csóka I, Erös I (2001) Interaction between liposomes and neutral polymers: effect of adsorption on drug release. J Dispersion Sci Technol 22:46–472. https://doi.org/10.1081/DIS-100107855
26. Savva M, Torchilin VP, Huang L (1999) Effect of polyvinyl pyrrolidone on the thermal phase transition of 1, 2 dipalmitoyl-sn-glycero-3-phosphocholine bilayer. J Colloid Interface Sci 217:160–165. https://doi.org/10.1006/jcis.1999.6343
27. Ariga K, Shin JS, Kunitake T (1995) Interaction of lipid monolayers with aqueous neutral polymers and the consequent monolayer stabilization and improved Langmuir-Blodgett transfer. J Colloid Interface Sci 170:440–448. https://doi.org/10.1006/jcis.1995.1123
28. da Silva RLCG, da Silva HFO, da Silva Gasparotto LH, Caseli L (2018) How the interaction of PVP-stabilized Ag nanoparticles with models of cellular membranes at the air-water interface is modulated by the monolayer composition. J Colloid Interface Sci 512:792–800. https://doi.org/10.1016/j.jcis.2017.10.091
29. Owen J, Kuznecovs M, Bhamji R, William N, Domenech-Garcia N, Hesler M, Knoll T, Kohl Y, Nelson A, Kapur N (2020) High-throughput electrochemical sensing platform for screening nanomaterial–biomembrane interactions. Rev Sci Instrum 91:025002. https://doi.org/10.1063/1.5131562
30. Coldrick Z, Penezić A, Gašparović B, Steenson P, Merrifield J, Nelson A (2011) High throughput systems for screening biomembrane interactions on fabricated mercury film electrodes. J Appl Electrochem 41:939–949. https://doi.org/10.1007/s10800-011-0319-7
31. Miller IR, Rishpon J, Tenenbaum A (1976) Electrochemical determination of structure and interactions in spread lipid monolayers. Bioelectrochem Bioenerg 3:528–542. https://doi.org/10.1016/0302-4598(76)80043-8
32. Nelson A, Benton A (1986) Phospholipid monolayers at the mercury/water interface. J Electroanal Chem Interf Electrochem 202:253–270. https://doi.org/10.1016/0022-0728(86)90123-3
33. Nelson A (2010) Electrochemistry of mercury supported phospholipid monolayers and bilayers. Curr Opin Colloid Interf Sci 15:455–466. https://doi.org/10.1016/J.COCIS.2010.07.004
34. Nelson A (2001) Conducting gramicidin channel activity in phospholipid monolayers. Biophys J 80:2694–2703. https://doi.org/10.1016/S0006-3495(01)76238-8
35. Moncelli MR, Becucci L, Nelson A, Guidelli R (1996) Electrochemical modeling of electron and proton transfer to ubiquinone-10 in a self-assembled phospholipid monolayer. Biophys J 70:2716–2726. https://doi.org/10.1016/S0006-3495(96)79841-7
36. Nelson A, Leermakers FAM (1990) Substrate-induced structural changes in electrode-adsorbed lipid layers: experimental evidence from the behaviour of phospholipid layers on the mercury-water interface. J Electroanal Chem Interfacial Electrochem 278:73–83. https://doi.org/10.1016/0022-0728(90)85124-N
37. Brukhno AV, Akinshina A, Coldrick Z, Nelson A, Auer S (2011) Phase phenomena in supported lipid films under varying electric potential. Soft Matter 7:1006–1017. https://doi.org/10.1039/c0sm00724b
38. Vakurov A, Galluzzi M, Podesta A, Gamper N, Nelson AL, Connell SD (2014) Direct characterization of fluid lipid assemblies on mercury in electric fields. ACS Nano 8:3242–3250. https://doi.org/10.1021/NN4037267
39. Mohamadi S, Tate DJ, Vakurov A, Nelson A (2014) Electrochemical screening of biomembrane-active compounds in water. Anal Chim Acta 813:83–89. https://doi.org/10.1016/J.ACA.2014.01.009
40. William N, Nelson A, Gutsell S, Hodges G, Rabone J, Teixeira A (2019) Hg-supported phospholipid monolayer as rapid screening device for low molecular weight narcotic compounds in water. Analytica Chimica Acta 1069:98–107. https://doi.org/10.1016/J.ACA.2019.04.019
41. Ormategui N, Zhang S, Loinaz I, Brydson R, Nelson A, Vakurov A (2012) Interaction of poly (N-isopropylacrylamide)(pNIPAM) based nanoparticles and their linear polymer precursor with phospholipid membrane models. Bioelectrochemistry 87:211–219. https://doi.org/10.1016/J.BIOELECHEM.2011.12.006
42. Vakurov A, Brydson R, Nelson A (2012) Electrochemical modeling of the silica nanoparticle–biomembrane interaction. Langmuir 28:1246–1255. https://doi.org/10.1021/LA203568N
43. Coldrick Z, Steenson P, Millner P, Davies M, Nelson A (2009) Phospholipid monolayer coated microfabricated electrodes to model the interaction of molecules with biomembranes. Electrochim Acta 54:4954–4962. https://doi.org/10.1016/j.electacta.2009.02.095
44. Rashid A, Vakurov A, Nelson A (2015) Role of electrolyte in the occurrence of the voltage induced phase transitions in a dioleoyl phosphatidylcholine monolayer on Hg. Electrochim Acta 155:458–465
45. Kohl Y, William N, Elje E, Backes N, Rothbauer M, Srancikova A, Rundén-Pran E, El Yamani N, Korenstein R, Madi L, Barbul

A et al (2023) Rapid identification of *in vitro* cell toxicity using an electrochemical membrane screening platform. Bioelectrochemistry 153:108467. https://doi.org/10.1016/j.bioelechem.2023.108467
46. Becucci L, Martinuzzi S, Monetti E, Mercatelli R, Quercioli F, Battistel D, Guidelli R (2010) Electrochemical impedance spectroscopy and fluorescence lifetime imaging of lipid mixtures self-assembled on mercury. Soft Matter 6:2733–2741. https://doi.org/10.1039/b923895f
47. Becucci L, Guidelli R, Polo F, Maran F (2014) Interaction of mixed-ligand monolayer-protected Au144 clusters with biomimetic membranes as a function of the transmembrane potential. Langmuir 30:8141–8151. https://doi.org/10.1021/la500909j
48. Wang X, Ma S, Su Y, Zhang Y, Bi H, Zhang L, Han X (2015) High impedance droplet–solid interface lipid bilayer membranes. Anal Chem 87:2094–2099. https://doi.org/10.1021/AC502953V
49. Vakurov A, Drummond-Brydson R, William N, Sanver D, Bastús N, Moriones OH, Puntes V, Nelson AL (2022) Heterogeneous rate constant for amorphous silica nanoparticle adsorption on phospholipid monolayers. Langmuir 38:5372–5380. https://doi.org/10.1021/acs.langmuir.1c03155
50. Ghosal PS, Gupta AK (2017) Determination of thermodynamic parameters from Langmuir isotherm constant-revisited. J Mol Liq 225:137–146. https://doi.org/10.1016/j.molliq.2016.11.058
51. Allen TE, Goodman JM, Gutsell S, Russell PJ (2014) Defining molecular initiating events in the adverse outcome pathway framework for risk assessment. Chem Res Toxicol 27:2100–2112. https://doi.org/10.1021/tx500345j
52. Qiu P, Mao C (2010) Biomimetic branched hollow fibers templated by self-assembled fibrous polyvinylpyrrolidone structures in aqueous solution. ACS Nano 4:1573–1579. https://doi.org/10.1021/nn9009196
53. Latour RA (2020) Fundamental principles of the thermodynamics and kinetics of protein adsorption to material surfaces. Colloids Surf B Biointerf 191:110992. https://doi.org/10.1016/j.colsurfb.2020.110992
54. Arumughan V, Nypelö T, Hasani M, Larsson A (2021) Fundamental aspects of the non-covalent modification of cellulose via polymer adsorption. Adv Coll Interface Sci 298:102529. https://doi.org/10.1016/j.cis.2021.102529
55. Reid MS, Villalobos M, Cranston ED (2017) The role of hydrogen bonding in non-ionic polymer adsorption to cellulose nanocrystals and silica colloids. Curr Opin Colloid Interface Sci 29:76–82. https://doi.org/10.1016/j.cocis.2017.03.005

Publisher's Note Springer Nature remains neutral with regard to jurisdictional claims in published maps and institutional affiliations.